Biomicrofluidics ARTICLE scitation.org/journal/bmf

Generation of functional hepatocyte 3D discoids in an acoustofluidic bioreactor

Cite as: Biomicrofluidics 13, 014112 (2019); doi: 10.1063/1.5082603
Submitted: 22 November 2018 · Accepted: 31 January 2019 ·
Published Online: 12 February 2019

Mogibelrahman M. S. Khedr,[1,2,a)] Walid Messaoudi,[3] Umesh S. Jonnalagadda,[3] Ahmed M. Abdelmotelb,[1,4] Peter Glynne-Jones,[3] Martyn Hill,[3] Salim I. Khakoo,[1,5] and Mohammed Abu Hilal[1,5]

AFFILIATIONS

[1]Clinical and Experimental Sciences Academic Unit, Faculty of Medicine, University of Southampton, Southampton SO16 6YD, United Kingdom
[2]Faculty of Medicine, Suez Canal University, Ismailia 41111, Egypt
[3]Mechanical Engineering, Faculty of Engineering and Physical Sciences, University of Southampton, Southampton SO17 1BJ, United Kingdom
[4]Faculty of Medicine, Tanta University, Tanta 31527, Egypt
[5]Southampton University Hospitals NHS Trust, Southampton SO16 6YD, United Kingdom

[a)]**Author to whom correspondence should be addressed:** M.E.Khedr@soton.ac.uk. **Tel.:** +44 (0) 2381206153.
Mob: +44 (0) 7961762098.

ABSTRACT

Ultrasonic standing wave systems have previously been used for the generation of 3D constructs for a range of cell types. In the present study, we cultured cells from the human hepatoma Huh7 cell line in a Bulk Acoustic Wave field and studied their viability, their functions, and their response to the anti-cancer drug, 5 Fluorouracil (5FU). We found that cells grown in the acoustofluidic bioreactor (AFB) expressed no reduction in viability up to 6 h of exposure compared to those cultured in a conventional 2D system. In addition, constructs created in the AFB and subsequently cultured outside of it had improved functionality including higher albumin and urea production than 2D or pellet cultures. The viability of Huh7 cells grown in the ultrasound field to 5FU anti-cancer drug was comparable to that of cells cultured in the 2D system, showing rapid diffusion into the aggregate core. We have shown that AFB formed 3D cell constructs have improved functionality over the conventional 2D monolayer and could be a promising model for anti-cancer drug testing.

INTRODUCTION

Hepatocellular carcinoma cell (HCC) lines including Huh7, cultured in 2D systems, show substantial loss of their xenobiotic-metabolizing enzyme activity and liver cell markers in contrast to 3D-organized cells which significantly express higher levels of differentiation markers and exhibit function closer to mature liver cells.[1–3] In addition, the culturing of cancer cells in a 3D model has the advantage of mimicking the *in vivo* tumour cell architecture and reflecting the proliferation pattern, apoptosis, oxygen/nutrient distribution, and the cell cycle heterogeneity of a tumour mass.[4,5]

The production of cell aggregates to simulate *in vivo* cell structure has been a major focus for biology, especially for *in vitro* drug testing.[6] Studies suggest that acoustic wave traps open potential applications for cell tissue engineering. Two main types of technology are used for exciting acoustic waves: Surface Acoustic Wave (SAW) and Bulk Acoustic Wave (BAW), both allowing a scaffold free aggregation of cells in a 3D structure.[7] BAW manipulation device typically consists of a resonator,[8,9] where a transducer excites a planar resonance in a fluid chamber [Fig. 1(a-i)]. A thickness acoustic standing wave is created within the cavity, the resulting radiation force pushing cells toward the pressure node which is located in the middle of the fluid cavity, allowing levitation[8] [Fig. 1(a-ii)], and also inter-particle (or Bjerknes) forces, attracting cells together into aggregates [Fig. 1(a-iii)].[10]

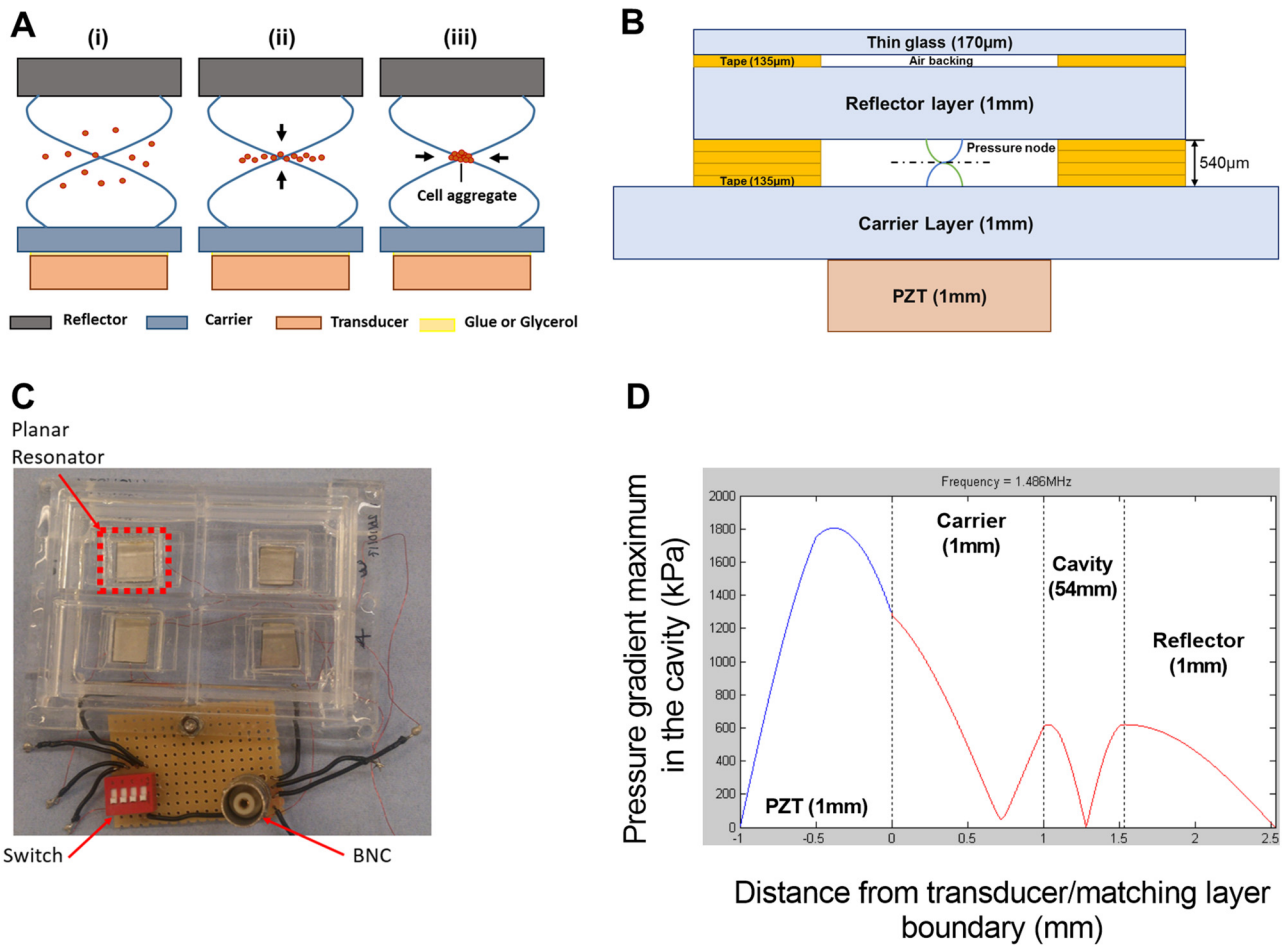

FIG. 1. Bioreactor design, fabrication, and modeling. (a) Planar resonator. (i) Acoustic standing wave in a planar resonator formed from reflections in the cavity of waves created by a transducer. (ii) This standing wave creates a time average acoustic energy gradient that "pushes" the particle to the pressure node (or kinetic energy maximum). (iii) Bjerknes forces aggregate the particles in a lump. (b) Schematic diagram detailing the planar resonator structure and dimensions. (c) Picture of the bioreactor showing the four resonator compartments and electrical connections. (d) Acoustic pressure amplitude in kPa in the layered resonator predicted by a transfer impedance model.

We describe the use of controllable cell aggregate formation in an acoustofluidic bioreactor (AFB) as a model for drug testing. The main benefits of contactless acoustic aggregation are the possibility of controlled mechanical stimulation induced by the force field;[11] the possibility of acoustic streaming to promote nutrient exchange with the surrounding media;[12] the ease of use; and finally, low energy and material costs.

In the present study, we have demonstrated the ability of a BAW mediated AFB system to form viable Huh7 cell aggregates in a short time. The Huh7 discoids we created possessed a substantial increase in the production of albumin and urea in addition to higher enzyme activity than the conventional 2D monolayer or pellet cultures. We have used 5 Fluorouracil (5FU), a cytostatic/cytotoxic anti-cancer agent that is commonly used for the treatment of solid tumours. 5FU resulted in a wide range of effects from the inhibition of cell proliferation to the induction of apoptosis and cell necrosis.[13,14] The AFB cell aggregates showed a robust susceptibility to the 5FU as compared to 2D controls.

MATERIALS AND METHODS

Bioreactor design, fabrication, and culture environment

The bioreactors used in the current study were fabricated according to the model that has been described by Jonnalagadda *et al.*[11] That bioreactor is a one-chamber device with a capacity of about 12 ml medium. We have used that model in investigating the Huh7 cell line viability and in performing the morphological studies. As seen in Figs. 1(b) and 1(c),

we have fabricated another four-chamber device, where every independent planar resonator has its own well (with a capacity of 1-2 ml medium) and that allowed running of four independent experiments in one device. The chamber spacer material was also changed to four layers of laser cut adhesive tape (3M 9731) to ease fabrication; however, the acoustic properties are not expected to differ as a result of this. This four-chamber model has been used for the rest of our studies.

Figure 1(d) shows the expected pressure distribution as modeled by a transfer impedance model[15] with a KLM transducer representation.[16] The bioreactor consists of four independently fabricated planar resonators (±5 μm in thickness and ±100 μm lateral arrangement) with each having its own fluidic well. Small manufacturing variations cause variability in the resonant frequency of each well. To hit the resonance frequency for each of them from a single source, a frequency sweep from 1.44 MHz to 1.51 MHz at a rate of 20 Hz is used. The voltage drop method was used to assess the acoustic pressure amplitude in the levitation cavity.[17] The acoustic pressure amplitude varies during the applied frequency sweep as the resonance is approached. By using the voltage drop method with the frequency sweep, we established that the mean force on particles (at the 7 Vpp driving amplitude, measured at the resonance frequency since the voltage varies across the sweep too) is equivalent to the force that would arise from a 380 kPa amplitude standing wave of constant amplitude. This is comparable to other acoustofluidic bioreactors.[18,19] Temperature rises within the chamber (caused by acoustic absorption) were measured by a thermocouple located inside and at the center of the planar resonator cavity and were found to be 2.4 ± 0.3 °C. The temperature rise attains 80% of its maximum value in around 5 min. The aggregation is not performed in an incubator, so the small rises in temperature above room temperature will not have a significant effect on viability.

Cell culture

The human hepatoma Huh7 cell line was a kind gift from Dr. A. Emre Sayan, Cancer Sciences Academic Unit, University of Southampton, UK. A Short Tandem Repeat (STR) analysis to verify the cell line identity was regularly performed. Cells were routinely cultured in Dulbecco's Modified Eagle Medium (DMEM) (Thermo Fisher, Inchinnan, UK) supplemented with 10% heat-inactivated fetal bovine serum (FBS) (Thermo Fisher), 100 U ml^{-1} of penicillin, 100 μg ml^{-1} of streptomycin, and 250 ng ml^{-1} of Gibco Amphotericin B. Cells were maintained at 37 °C in a humidified incubator with 5% CO_2 and the medium was changed every three days.

Cells were detached using non-enzymatic cell dissociation buffer (Sigma), washed once with complete medium and centrifuged at 250*g* for 5 min. Cell pellet was aliquoted into three populations; one cell aliquot was re-centrifuged as before and cell pellet was maintained in a 15 ml tube as the pellet culture. Another aliquot was seeded directly in a 12 well plate, and the third aliquot was loaded into AFB bioreactor. In anti-cancer drug testing, cells were loaded in the AFB for 2 h after which the generated discoids were transferred to 1% agarose coated 24 well plates. Following 24 h, AFB discoids or cells cultured in the 2D monolayer or as pellets were treated with serial 10-fold dilutions (1, 10, or 100 μM) of 5 Fluorouracil (5FU) (Sigma, Gillingham, UK) dissolved in dimethyl sulfoxide (DMSO) (Sigma). Negative control cells were treated with medium with DMSO alone. Supernatants were aspirated daily and replaced with new treatment medium for three subsequent days.

Viability and morphology of Huh7 in AFB

Cell viability was assessed by a live/dead staining technique. Calcein AM (Thermo Fisher) and Propidium Iodide (PI) (1-3 μM final concentrations of each) were added to medium following incubation of cells in the 2D monolayer or AFB cultures at room temperature. Imaging was performed in a Zeiss-microscope using AxioVision SE64 version 4.9.1 software. Viability was expressed as the percentage of viable cell area to the total cell area using Fiji version of ImageJ software for windows.[20] Viability was calculated in five different fields per condition in three independent experiments. For studying the aggregates' morphology, cells were incubated in medium with 5 μM CellTracker™ Green CMFDA Dye (Thermo Fisher) for 30 min and then loaded into the AFB at a density of 10^6 cells ml^{-1} for 1 h. Cell aggregates were recovered and imaged with a Leica TCS-SP8 Laser Scanning Confocal Microscope (Leica Biosystems, Wetzlar, Germany).

Detection of E-cadherin in Huh7 by western blotting

Huh7 were cultured as the 2D monolayer, pellet, or in AFB for 1/2, 1, 3, 6, and 16 h. Cells were lysed using 1× TruPAGE™ LDS Sample Buffer [with 1 mM ethylenediaminetetraacetate (EDTA), 1 mM ethylene glycol-bis (β-aminoethyl ether)-N,N,N′, N′-tetraacetic acid (EGTA) (Sigma), and 0.5 μg ml^{-1} Leupeptin] and run a TruPAGE® 10% precast gels (Sigma) with TruPAGE dithiothreitol (DTT) sample reducer buffer (Sigma) to disrupt the disulphide bridges in proteins which liberate small polypeptides. Protein was loaded in a concentration of 30 μg as adjusted by the bicinchoninic acid (BCA) colorimetric protein assay kit (Sigma) in accordance with the manufacturer's instructions using a BSA standard. Molecular weights were determined using the PageRuler™ Plus prestained protein ladder, 10-250 kDa (Thermo Fisher). Proteins were transferred to nitrocellulose membranes by a wet transfer method. Membranes were blocked for 1 h in 5% non-fat blotting grade cow's milk (Bio-Rad) in 0.05% Tris-buffered saline (TBS)—Tween® 20 solution. The membranes were then probed with 1 μg ml^{-1} mouse monoclonal anti-human E-cadherin IgG2B antibody Clone #180224 (R&D Systems, Oxfordshire, UK) overnight at 4 °C, followed by rabbit polyclonal anti-mouse-horseradish peroxidase (HRP) (DakoCytomation, Cambridgeshire, UK) at a dilution of 1:2000 for 45 min. Membranes were probed with mouse monoclonal anti-β-actin-HRP conjugated (Sigma) for 1 h at room temperature at a dilution of 1:50 000. Reactive bands were visualised using the Luminata Forte Western

HRP substrate chemiluminescent substrate (Millipore UK Ltd., Hertfordshire, UK) in a ChemiDoc™ imaging system (Bio-Rad).

Albumin ELISA and urea concentration assays

Albumin and urea concentrations in the supernatant of hepatocytes cultures were determined using the ELISA DuoSET® kit for human albumin (R&D Systems, Oxfordshire, UK) according to the manufacturer's instructions. Urea concentration was measured as described previously.[21] Briefly, the urea reagent mix working concentrations of 100 mg l^{-1} o-phthalaldehyde, 513 mg l^{-1} primaquine bisphosphate, 2.5 mol l^{-1} sulfuric acid, 2.5 g l^{-1} boric acid, and 0.03% Brij-35 were prepared. A volume of 200 μl freshly prepared reagent mix was added to 50 μl samples or standard (QuantiChrom, BioAssay Systems, Hayward, CA, USA). Following 1 h incubation at room temperature, absorbance at 430 nm was measured in a SpectraMax® Plus 384 Microplate Reader (Molecular Devices, Wokingham, UK). The concentration of urea of the sample against 5 mg dl^{-1} standard was calculated in mg dl^{-1}.

CYP3A4 activity assay

Cytochrome P450 3A4 (CYP3A4) activity in Huh7 in different cultures was measured using a P450-Glo™ CYP3A4 Assay (Luc-PFBE) Cell-Based/Biochemical luminescent assay (Promega UK Ltd, Southampton, UK) according to manufacturer's instructions. Briefly, Huh7 cells were cultured for various time periods in different culture systems then basal CYP3A4 enzyme activity was assessed by incubating cells with luminogenic P450-Glo substrate (luciferin-PFBE, at a final concentration of 50 μM) for 3 h at room temperature. The luciferin was detected by incubating 25 μl of supernatant with an equal volume of Luciferin Detection in a white opaque 96 well plate for 20 min at room temperature. Light was measured in a FLUOstar OPTIMA plate reader (BMG LABTECH, Ortenberg, Germany). Values have been corrected to the corresponding time course cell viability in various culture systems.

Analysis of apoptosis in Huh7 using a DNA fragmentation assay

Huh7 grown in various culture systems and those treated with 5FU (1, 10, and 100 μM) for various time points were investigated for possible induction of apoptosis using the DNA degradation assay as described.[22] Cells were lysed using 20 μl TES lysis buffer [100 mM Tris, pH 8.0 + 20 mM EDTA + 0.8% (w/v) sodium dodecyl Sulfate (SDS)] and then incubated for 30-120 min at 37 °C with 10 μl of RNase A at a concentration of 500 units ml^{-1}. DNA was extracted using proteinase K (20 μl of 10 mg ml^{-1}) overnight at 50 °C in a heat block and ladder formation was explored by running DNA on a 1% agarose gel at 35 V for 4 h. Quantification of bands was performed by Image Lab version 5.2.1 software using Bio-Rad's ChemiDoc Imaging Systems System (Bio-Rad Laboratories, Hercules, CA, USA).

Cell proliferation assay

Huh7 grown in various culture systems and treated with 5FU (1, 10, and 100 μM) for 24, 48, and 72 h. Cell growth was determined using a colourimetric Quick Cell Proliferation Assay kit II (Abcam, Cambridge, UK) according to manufacturers' instructions. Briefly, lyophilized water-soluble tetrazolium salt (WST-1) reagent was dissolved into 5 ml Electro Coupling Solution (ECS) and the solution stored at −20 °C. Ten microliters of WST-1 solution was added to the medium and cells were incubated in standard culture conditions for 3 h. Absorbance was detected at 440 nm.

Measurement of lactic dehydrogenase (LDH)

LDH levels in supernatants from Huh7 were grown in various culture systems and treated with 5FU (1, 10, and 100 μM) for 24, 48, and 72 h. Equal volumes of 200 mM Tris pH 8, 50 mM Lithium lactate, freshly prepared substrate solution [100 μl P-Iodonitrotetrazolium Violet, INT (33 mg ml^{-1} in DMSO) + 100 μl, Phenazine methosulfate, PMS (9 mg ml^{-1}) + 2.3 ml β-NAD hydrate (3.74 mg ml^{-1})] and supernatants samples or positive control (5 μg ml^{-1} L-Lactic Dehydrogenase from bovine heart) (Sigma) were loaded into an assay plate. The V_{max} was measured at 490 nm for 10 min and LDH activity (U ml^{-1}) was calculated.

Statistics

One-way or two-way ANOVA followed by Fisher's least significant difference (LSD) multiple comparisons tests and multiple or paired Student's t tests were performed using GraphPad Prism version 7.7.1 for Windows (GraphPad Software, La Jolla, CA, USA).

RESULTS

Generation of Huh7 discoids in an AFB

The size of cell aggregates has been shown to have a strong impact on cellular viability and function.[23] The uniformity of aggregates size is critical for the validity of chemotherapeutic drug screening. We investigated the size of discoids formed by injecting Huh7 cell suspensions of variable cell densities into the AFB. Huh7 cells were observed to aggregate over the course of 15 min following cell injection [Fig. 2(a) (Multimedia view)]. Typically, 9-12 discoids were formed corresponding to the acoustic trapping locations. At a density of 0.25×10^6 cells ml^{-1}, small Huh7 cell aggregates were formed (with a mean diameter of 381.6 ± SD 113 μm) and there was a little increase in discoid size at density of 0.5×10^6 cells ml^{-1} [Fig. 2(b)]. The size of discoids was markedly increased at a seeding density of 1.25×10^6 cells ml^{-1} (a mean diameter of 525.4 ± SD 118.7 μm, $P < 0.0001$) and larger discoids were generated at higher cell densities (a mean diameter of 1021 ± SD 267.8 μm, $P < 0.0001$ and 1382 ± SD 403.1 μm, $P < 0.0001$ at a cell density of 2.5×10^6 and 5×10^6 cells ml^{-1}, respectively). Up to 5×10^6 cells ml^{-1}, there was no marked change in size along the z (i.e., the sound propagation) axis.

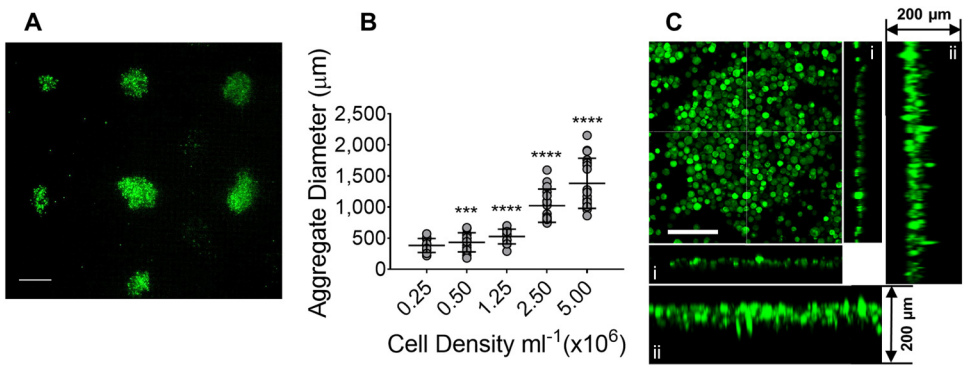

FIG. 2. Size of Huh7 discoids generated in acoustofluidic bioreactor (AFB). [(a) and (Multimedia view)] Huh7 discoids formed at a density of 1.25×10^6 cells ml^{-1} in AFB. Cells were pre-labeled with calcein AM and loaded for 30 min in the AFB. Scale bar = 500 μm. (b) Aggregate diameter (μm) was plotted against cell density (n = 3). *P* values shown in the graph are for the comparison to a cell density of 2.5×10^5 cells ml^{-1}. ***$P = 0.0001$, ****$P < 0.0001$. Mean ± SD. One-way ANOVA followed by Fisher's least significant difference (LSD) test. (c) Orthogonal projection of Huh7 showing a discoid shaped cell aggregate. A 200 μm z projection was demonstrated and showing x and y axes without (i) or with maximum projection (ii). Cells at a density of 10^6 cells ml^{-1} were labeled with CellTracker Green CMFDA Dye and incubated in the AFB for 1 h. Scale = 100 μm. Multimedia view: https://doi.org/10.13039/501100000266

Cells were unevenly aggregated laterally, creating a multitude of discoids levitating in the same plane with thickness ranging from 20 to 60 μm [i.e., one to three cell layers, Fig. 2(c-i) and 2(c-ii)]. In a previous report, Chen *et al.* showed that the diameter of spheroids could depend on the density of cells in the medium and wavelength of standing wave.[24] Although the generated discoids in our system do not correspond to Chen's model, the overall volume of the discoids has altered with the change of density of cells in the medium while the thickness of the discoids does not change with density. The thickness of cell discoids was similar between the center and periphery of the cell aggregates. Cell discoids formed at a cell density of 1.25×10^6 cells ml^{-1} showed the least variability in size and therefore this cell density has been used in the subsequent experiments. The wavelength at the frequency used in our experiments was 1 mm in the filled cavity, which allowed the generation of large sized cell aggregates at high cell density.

In the absence of extracellular matrix, E-cadherin has been found to play a crucial role in cell-cell adhesion, maintenance of survival, and proliferation of cancer cell aggregates.[25] The role of E-cadherin adhesion molecules in AFB driven aggregate formation was investigated using western blotting. Huh7 single cell suspensions were found to express highly preserved E-cadherin molecules, while in the subsequent 2D monolayer or AFB cultures, E-cadherin was found to lose its integrity [Fig. 3(a)]. Seeding cells in an ultrasound field was observed to initiate a gradual cleavage of full length E-cadherin (120 kDa) into smaller fragments, mostly as C-terminal fragment 1, CTF1 (38 kDa) and to a lesser extent C-terminal fragment 4, CTF4 (23 kDa) and C-terminal fragment 2, CTF2 (33 kDa) [Fig. 3(b)]. Almost all E-cadherins underwent fragmentation following 3 h of cell aggregation in the AFB. On the other hand, E-cadherin was cleaved early in the course of the 2D monolayer cell culture [Fig. 3(c)]. Notably, cells in AFB cultures express more full length E-cadherin than those cultured as 2D monolayers, but there were no qualitative differences observed in fragments distribution in both cell cultures. These findings highlight the important role of E-cadherin in AFB induced cell-cell contact and aggregate formation. As E-cadherin promotes a calcium-dependent cell-cell adhesion,[26] the interference of E-cadherin assembly was tested by adding a selective calcium chelator (EGTA) to the culture medium. The presence of 10 mM EGTA in the culture medium was found to inhibit cell aggregation in the AFB [Fig. 3(d)], which suggests that calcium-dependent adhesion molecules contribute to discoid formation in the AFB.

Viability and functions of Huh7 in the AFB environment

The influence of the AFB on the viability and function of Huh7 was next investigated. The viability of Huh7 was detected by labeling cells with calcein AM and PI following incubation in the 2D monolayer or AFB cultures at room temperature [Fig. 4(a)]. It was found that the viability of Huh7 decreased to an average of 43.3% and 46.94% for 2D and AFB, respectively, at the previous conditions, and to 31.7%, $P = 0.1807$ and 23.92%, $P = 0.0111$ for 2D and AFB, respectively, at 3 h of incubation and was dramatically reduced to only 3.46%, $P = 0.0003$ and 8.72%, $P = 0.0002$ for 2D and AFB, respectively, after 6 h [Fig. 4(b)]. No marked differences were observed between the 2D monolayer and AFB cultures. Culture of Huh7 cells in DMEM culture medium buffered with [4-(2-hydroxyethyl)-1-piperazineethanesulfonic acid] (HEPES) (Thermo Fisher) showed an initial high cell viability of 94.11% and 98% following 30 min culture in 2D and AFB systems, respectively [Fig. 4(c)]. The viability of cells was found to be preserved at 83.35%, $P = 0.3438$ and 81.86%, $P = 0.1078$ for 2D and AFB, respectively, after 6 h of culture. No marked

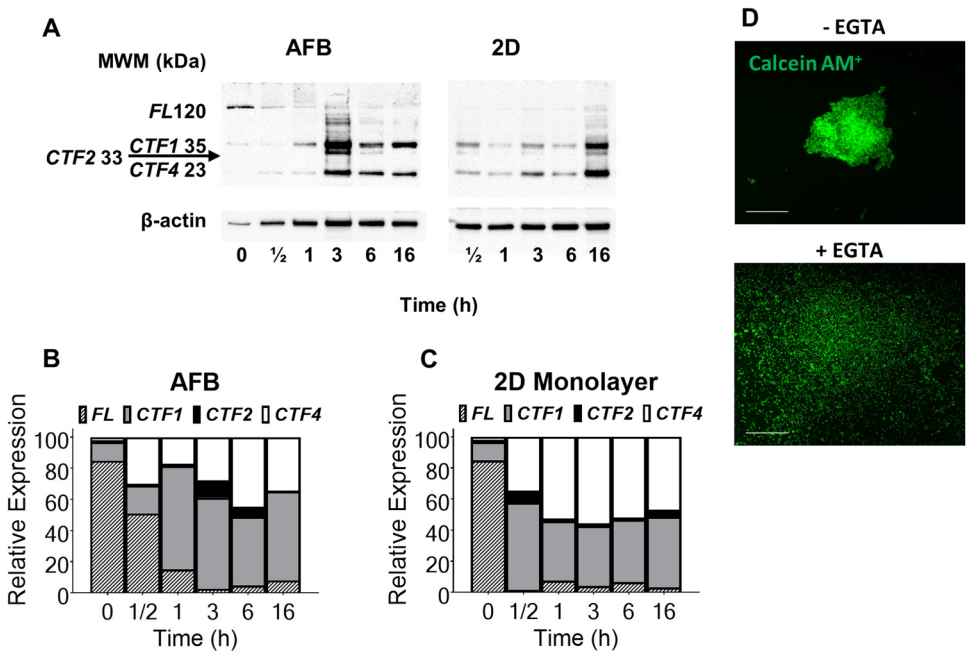

FIG. 3. Detection of E-cadherin expression in Huh7 using western blotting technique. (a) Representative blot for detection of E-cadherin protein expression in Huh7 grown as the 2D monolayer or in AFB (0 time point represents single cell suspension just before seeding). Molecular weight marker (MWM) is indicated. E-cadherin Full length, FL (120 kDa), C-terminal fragment 1, CTF1 (38 kDa), C-terminal fragment 2, CTF2 (33 kDa), and C-terminal fragment 4, CTF4 (23 kDa) are indicated. [(b) and (c)] Band density analysis (band intensity normalised to β-actin control) of E-cadherin fragments detected by western blotting in Huh7 cells cultured in AFB or 2D systems, respectively. (d) Effect of calcium chelation on AFB induced cell aggregates. Huh7 aggregate formation was observed using usual medium (without EGTA, −EGTA) or with 10 mM EGTA (+EGTA) in AFB for 3 h. Cells were labeled with calcein AM (green) before loading. Scale = 500 μm.

difference in cell viability was observed between the two culture methods.

The synthetic and metabolic functions of Huh7 cells were tested in the AFB with time course experiments and compared to the conventional 2D monolayer and 3D pellet cultures. Cells cultured in the AFB showed a time dependent increase in albumin secretion in the cell culture supernatant [Fig. 5(a)]. The albumin concentration rose to a mean of 11.02 ± SEM 2.18 ng ml^{-1} after 6 h in the AFB which is nearly double that after 30 min in the trap (a mean of 2.24 ± SEM 0.79 ng ml^{-1}, $P < 0.0001$). A similar pattern was observed with cells seeded as 2D monolayers (means of 5.62 ± SEM 0.85 ng ml^{-1}, $P = 0.0002$ and 11.48 ± SEM 0.87 ng ml^{-1}, $P < 0.0001$ at 3 and 6 h, respectively, compared to that after 30 min incubation). In contrast, pellet-cultured Huh7 did not show a marked increase in albumin levels (means of 4.67 ± SEM 0.91 ng ml^{-1}, $P = 0.0324$ and 6.74 ± SEM 0.434 ng ml^{-1}, $P = 0.0341$ at 3 and 6 h, respectively, compared to that after 30 min incubation). Albumin secretion from cells in both AFB and 2D cultures was markedly higher than that released from cells cultured as pellets. In addition, a noticeable increase in albumin levels was detected in the AFB system when compared to that observed in the 2D monolayer in the first hour of cell culture (means of 8.62 ± SEM 1.35 and 5.98 ± SEM 0.78 ng ml^{-1}, respectively, $P = 0.0078$).

Huh7 cells cultured in the AFB had a time dependent increase in urea secretion with a mean of 6.95 ± SEM 0.04 mg dl^{-1} following 6 h in culture from a baseline of 6.05 ± SEM 0.05 mg dl^{-1} at 30 min [Fig. 5(b)]. Similarly, cells in 2D culture were found to produce more urea following 6 h in culture (a mean of 6.19 ± SEM 0.67 mg dl^{-1}), while cells cultured as pellets showed high urea production after 3 h of incubation (a mean of 6.16 ± SEM 0.07 and 6.12 ± SEM 0.05 mg dl^{-1} at 3 and 6 h, respectively). Urea production was found to be higher in cells cultured in the AFB system when compared to other culture systems at all-time points.

Cytochrome P450 3A4 (CYP3A4) enzyme is the principal and abundant isoform of human CYP3A family.[27] It has the widest catalytic selectivity and is responsible for the metabolism of about ~30%-40% of clinically used drugs.[28,29] In this study, we measured basal CYP3A4 activity using a luminescent substrate based enzyme assay as an indicator of the metabolic status of Huh7 cells in used cultures. Huh7 cells subjected to ultrasound waves in AFB for 30 min express low CYP3A4 activity but following 6 h of incubation, cells retrieved high enzyme activity (a mean of 1431.386 ± SEM 139.66 and 2233.77 ± SEM 242.88 RLU, respectively, $P = 0.0397$) [Fig. 5(c)]. There is no distinct difference in CYP3A4 activity between cells cultured in AFB or 2D monolayer

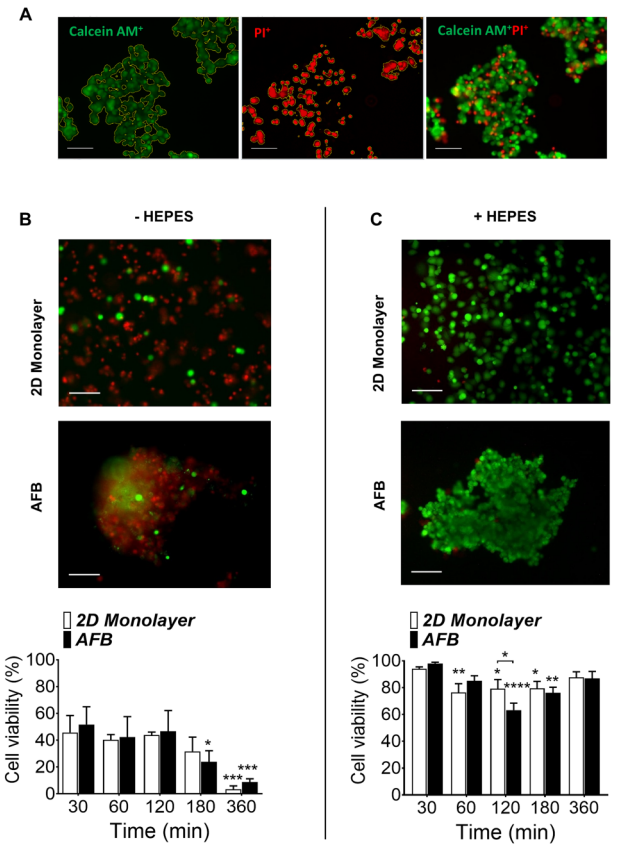

FIG. 4. Survival of Huh7 cells in the AFB. Live cells were labeled with calcein AM (green), and dead cells were labeled with Propidium Iodide (PI, red) in the (a) absence or (b) presence of 25 mM [4-(2-hydroxyethyl)-1-piperazineethanesulfonic acid] (HEPES) in culture medium. Representative images of cells following 360 min incubation in 2D or AFB system were presented and percentage of live cells were plotted against time of cell incubation. Scale bar = 100 μm. n = 3. *P* values shown in the graph are for comparison to 30 min time point (on top of bars). $^{*}P < 0.05$, $^{**}P < 0.005$, $^{***}P < 0.0005$, $^{****}P < 0.0001$. Mean ± SEM. Two-way ANOVA followed by Fisher's LSD test.

following 6 h and both cultures had higher enzyme activity compared to pelleted cells.

Acoustically driven microbubble cavitation and localised streaming are believed to play a role in ultrasound mediated cell membrane disruption (known as Sonoporation).[30,31] This results in an increase in cell membrane permeability and in the release of various intracellular molecules. Cell membrane permeability was tested using calcein AM. Calcein AM was readily taken up and converted by cytosolic esterase to calcein that gives an intense green florescence for viable cells with intact cell membrane.[32] We pre-loaded Huh7 cells with calcein AM dye and then monitored fluorescent intensity of calcein AM in cells at various time points in AFB [Fig. 5(d)]. Up to 6 h, cell exposure to ultrasound wave was not associated with any notable change of cell wall integrity as compared to cells cultured as 2D monolayers [Fig. 5(e)].

In the previous experiments, using the four-chamber device, with its limited volume capacity was associated with an impact on cell viability with time. Huh7 cells grown in AFB showed a higher percentage of dead cells (46.65% of total cells) at 6 h compared to cells grown in the 2D system (12.18% of total cells). A higher LDH activity was observed in Huh7 cells maintained for 6 h in the acoustic field (mean 20.48 ± SEM 6.59 U ml^{-1}) when compared to 2D or pellet cultures (mean of 5.71 ± SEM 0.75 and 3.63 ± SEM 0.66 U ml^{-1}, respectively) [Fig. 5(f)]. We found that medium levels in bioreactor wells were significantly decreased after 6 h and marked condensations were observed on the bioreactor lid. Loss of water from medium exposes cell to acute hyperosmolarity stress that may lead to cell apoptosis and death as describe before.[33,34] In contrast, we have shown previously that cell integrity has not been changed in the course of time when seeded in the one-chamber device, which accommodate larger volume of medium (see the Viability section). Potential stimulation of apoptosis in cultured Huh7 cells was investigated by DNA fragmentation. Cells did not show significant apoptotic DNA degradation in all three culture systems tested [Fig. 5(g)].

Anti-cancer drug testing

5 Fluorouracil (5FU) is a cytostatic antimetabolite drug that has been reported to inhibit cell growth and induce apoptosis in several HCC cell lines including Huh7.[13] AFB generated discoids were treated with various concentrations of 5FU and compared to cells cultured as 2D monolayers and pellet cultures. Drug dependent alteration of Huh7 viability was studied using a WST-1 salt cell proliferation assay. In the first 24 h of culture, more than half of the metabolically active cells died in the AFB and pellet cultures. However, deterioration of cell viability was not observed in cells grown as the 2D monolayer [Fig. 6(a)]. Interestingly, a dose dependent decrease in cell proliferation was observed after 48 h of 5FU treatment in cell aggregates formed in AFB (a mean of 7.90% ± SEM 2.20 lower than untreated cells) [Fig. 6(b)]. This decrease was higher in pellet cultures or 2D cultures (a mean of 24.88% ± SEM 4.76 and 14.71% ± SEM 4.90 lower than untreated cells, respectively) [Figs. 6(c) and 6(d)]. Following 72 h of anti-cancer treatment, Huh7 discoids generated in the AFB demonstrated a similar pattern of decline in their proliferation (a mean of 8.86% ± SEM 2.07 lower than untreated cells at 100 μM). At the same 5FU concentration, more growth inhibition was found in pelleted cells (a mean of 15.57% ± SEM 4.67 lower than untreated cells) but the decrease in cell growth in the conventional 2D culture was close to that noticed in AFB culture (a mean of 9.29% ± SEM 5.05 lower than untreated cells). Following 48 h culture, the growth inhibition of Huh7 was induced at lower concentrations of 5FU in 2D monolayers when compared to AFB [inhibitory concentration 50 (IC50) 1.96 and 5.54 μM, respectively], while the proliferation of cells cultured as pellets was inhibited at markedly higher concentrations (IC50 19.79 μM) [Fig. 6(e)]. The pattern of 5FU potency changed following 72 h as cell proliferation was inhibited at higher concentrations in 2D monolayers, while cells in the AFB did not

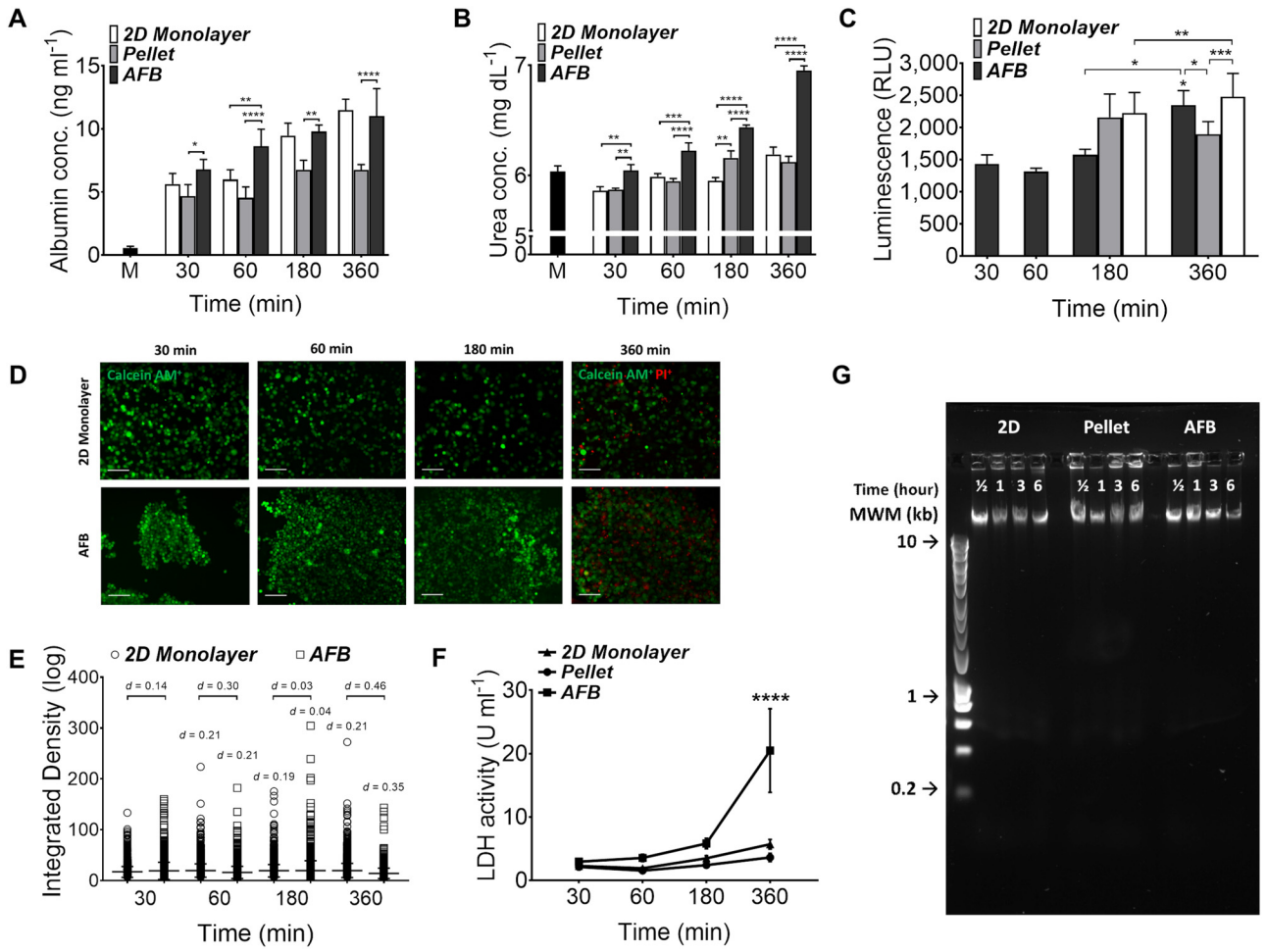

FIG. 5. Functions of Huh7 in the AFB. (a) Albumin concentrations (ng ml^{-1}) and (b) urea concentrations (mg dl$^{-1)}$ in supernatants from Huh7 cultured in the 2D monolayer, pellet, or AFB cultures with time course. n = 3. *P* values shown in the graph are for comparison to cells after 30 min between various cultures. M, medium. (c) CYP3A4 activity in Huh7 cultured in the AFB system with time course and following 3 and 6 h as the 2D monolayer or pellet cultures. n = 3. *P* values shown in the graph are for comparison to cells after 30 min in AFB or between various cultures. **P* < 0.05, ****P* < 0.0005, *****P* < 0.0001. Mean ± SEM. Paired Student *t* test. (d) Permeability of Huh7 with time course in AFB compared to the 2D monolayer culture with time course. Cells were preloaded with calcein AM (1 μM), scale = 100 μm and (e) quantification of change in cell fluorescence over time course, expressed as integrated density. Difference between means tested by Cohen's *d* effect size values were marked. Mean ± SD. *d* = 0.2 (small) and *d* = 0.5 (medium). (f) Lactic dehydrogenase (LDH) activity (U ml^{-1}) in supernatants from Huh7 cultures with time course. n = 3. *P* values shown in the graph are for comparison between various cultures with time course (on top of bars). *****P* < 0.0001. Mean ± SEM. Two-way ANOVA followed by Fisher's LSD test. (G) DNA fragmentation assay of Huh7 DNA loaded in 1% agarose gel with different culture systems and time (representative image of 3 experiments). HyperLadder™ 1 kb molecular weight marker (MWM) was indicated.

show a significant change in their response to 5FU (IC50 9.52 and 4.29 μM, respectively). Conversely, the proliferation of cells cultured as pellets was inhibited at much lower concentration (IC50 2 μM) [Fig. 6(f)]. To determine whether the decreased in cell survival was caused by blunting of cell growth or cell death, further calcein AM/PI viability and LDH activity assays were used.

Numbers of dead cells were increased in the AFB or pelleted cultures following 72 h of incubation with high concentrations of 5FU [Fig. 7(a)], whereas few dead cells were observed in the 2D monolayer. The reaction of cells grown in 2D monolayers seems to appear as an inhibition of proliferation rather than cell cytotoxicity. LDH release in supernatants of cell aggregates from AFB or pellet cultures showed higher basal levels [Fig. 7(b)]. A marked increase in LDH activity was been found in cells grown after 72 h incubation with 5FU at 100 μM in all cell cultures. A limited increase in LDH release was observed in cells cultured in AFB as compared to a 2D monolayer (a mean of 5.23 ± SEM 0.59 and 4.39 ± SEM 0.47 U ml^{-1}, respectively). Pelleted cells did show a higher

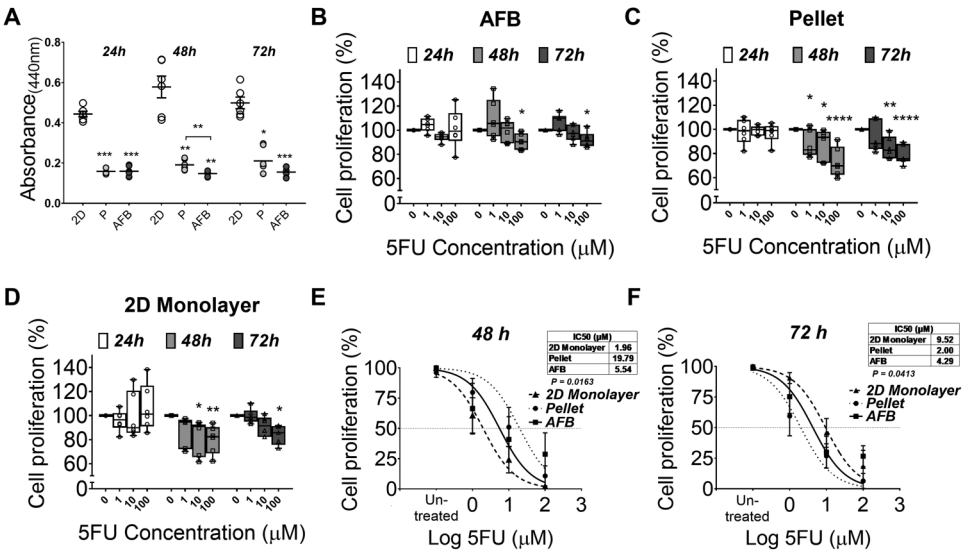

FIG. 6. Anticancer drug testing of Huh7 AFB generated discoids. Proliferation of Hhu-7 on various cell cultures (a) or following treatment with various concentrations of 5 Fluorouracil (5FU) cultured in (b) AFB, (c) pellet, or (d) 2D monolayer cultures with time course (expressed as percentage of un-treated cells). n = 3. *P* values shown in the graph are for comparison to un-treated cells. [(e) and (f)] Inhibitory concentration 50 (IC50) of 5FU in various culture conditions following 48 h or 72 h, respectively. $^{*}P < 0.05$, $^{**}P < 0.005$, $^{***}P < 0.0005$, $^{****}P < 0.0001$. Mean ± SEM. Two-way ANOVA followed by Fisher's LSD test.

LDH activity at all 5FU concentrations (a mean of 6.40 ± SEM 0.97 U ml^{-1}). Finally, the 5FU induction of apoptosis in Huh7 was explored by detecting the DNA fragmentation. DNA degradation in cell discoids generated in AFB was clear after 5FU treatment at concentrations of 10^2 and 10^3 μM [Fig. 7(c)]. The response of cells grown in the 2D monolayer was relatively less than that in AFB culture, but pellet culture showed responses only at a high concentration of 5FU (10^3 μM).

DISCUSSION

In the present study, we have investigated an acoustofluidic, matrix-free discoid aggregation system for Huh7 cells. In contrast to our previous work[11] with chondrocytes (which included 21 day levitated culture), the bioreactor was used only during an initial aggregate formation period of 6 h followed by the conventional culture in a well-plate. Following sonication, the Huh7 hepatoma cells have shown high viability and improved function in comparison to the conventional 2D monolayer culture. Moreover, exposure to ultrasound waves was associated with high levels of E-cadherin and an increase in proliferation in aggregated cells. The AFB fabricated cell aggregates were found to be suitable for anti-cancer drug testing and apoptosis assays.

The diameter of our disc-like aggregates was found to be dependent on cell density, while their thickness is relatively constant at a cell density up to 5×10^6 ml^{-1}. Bazou *et al.* have reported similar findings with the hepatoblastoma cell line, HepG2.[19] They noticed that at a density of 1×10^6 cells ml^{-1}, a 3D multilayer discoid cell aggregate formed which steadily increased in diameter with higher cell concentrations. In contrast to our results, they found an increase in aggregate thickness with higher cell densities and a tendency of cells to accumulate at the center of the discoid rather than its edges. However, the distribution of the lateral acoustic field of the Bazou device was significantly different, having a single kinetic energy density maximum, which attracted cells over an area many wavelengths in width, while in our device, multiple, smaller aggregates are formed, such that there is a different balance between axial and lateral components of the acoustic radiation force.

Cell-cell contact, spreading, and attachments were found to be initiated in the AFB, and these events cause stable aggregates. Huh7 cells express several adhesion molecules including E-cadherins,[3,35,36] which play a crucial role in hepatoma cell aggregate formation.[37] In the present study, we investigated the alteration of expression of E-cadherin in Huh7 in the AFB. Full length E-cadherin cell expression was higher in the AFB system than in the 2D monolayer culture that agrees with previous studies.[7,38] In these reports, ultrasound waves resulted in the accumulation of neural cell adhesion molecule (NCAM) and N-cadherin and induced re-organisation of F-actin accumulation of adhesion molecules markedly following 30 min of sonication. Initially, during the first 3 h of levitation in the AFB, cells appear to shift from cell suspension status where the preserved E-cadherin could potentially mediate cell aggregation to aggregates that may harbour proliferating cells, as evidenced by cleavage of E-cadherin. In fact, cleavage of E-cadherin is essential for tumour cell extrusion and proliferation.[39] In the case of 2D monolayers, limited cell contact could allow cells to

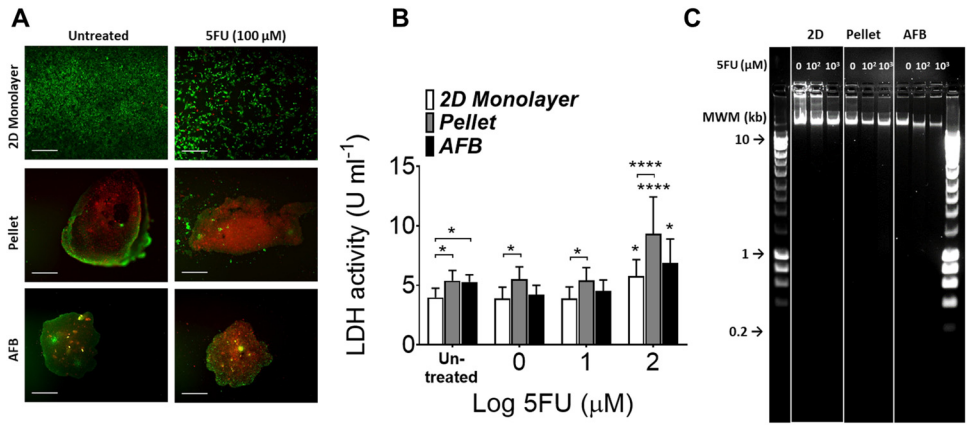

FIG. 7. 5FU induces cell death and apoptosis in Huh7 AFB generated discoids. (a) Live/dead staining of Huh7 cultured in the 2D monolayer, pellet, or AFB cultures 72 h following addition of 100 μM 5FU. Scale bar = 500 μm. (b) LDH (U ml^{-1}) release in supernatants from Huh7 cultured in various culture conditions 72 h following addition of 5FU. n = 3. *P* values shown in the graph are for comparison to untreated cells (on top of bars) or to the cell in the 2D monolayer culture. **P* < 0.05, ***P* < 0.005, ****P* < 0.0005, *****P* < 0.0001. Mean ± SEM. Two-way ANOVA followed by Fisher's LSD test. (c) DNA fragmentation assay of Huh7 DNA following treatment with 5FU loaded in 1% agarose gel with different culture systems (representative image of 3 experiments). HyperLadder 1 kb molecular weight marker (MWM) was indicated.

proliferate early in their culture. AFB Huh7 cell aggregation is suggested to be E-cadherin dependent, which could make this system a good tool for studying cadherin mediated pathways.

Physical stresses resulted from exposure to acoustic radiation forces such as changes in temperature and cavitation effects could influence cell viability and may lead to cell damage.[40] Cell viability was assessed using calcein AM/PI live/dead dyes and DNA degradation assays. We did not find a marked effect of the AFB system on cell viability or the induction of apoptosis after 6 h in the bioreactor compared to the 2D culture system controls. This was in agreement with reports showing that cells that had been levitated in acoustofluidic systems maintained their integrity.[41–43] Moreover, a notable stability of the gene expression profile has been described in cells such as embryonic stem cells exposed to ultrasonic standing waves with a pressure amplitude up to 0.85 MPa.[44] The cavitation effect depends on the peak negative pressure (in MPa) as well as the frequency of acoustic wave. The ratio of these two factors determines the cavitation threshold that expressed as the mechanical index (MI). Risk of cavitation could be avoided by keeping the MI lower than 1.[40] Our system provided an exposure of Huh7 cells to a pressure amplitude (and peak negative pressure) of 0.38 MPa at a frequency of 1.5 MHz. These conditions reduced the risk of cavitation by keeping MI at about ~0.3. Moreover, the used pressure amplitude is far less than that reported before by Bazou *et al.*[18] (i.e., 1.96 MPa) which produce cavitation. Indeed, cells showed an intact cell membrane with the retention of calcein AM which exclude the occurrence of cavitation in our AFB.

In the present study, we have shown that the incubation of Huh7 cells in the AFB was associated with an improvement of their ability to produce albumin and urea. These results are in agreement with those previously reported with HepG2 cells.[7,19] In addition, we have observed increased CYP3A4 enzyme activity which was previously reported.[2] Culturing of Huh7 in a confluent state or in a 3D system could dampen their proliferative drive and promote their metabolic efficiency.[2,45,46] However, our results are more consistent with an advantageous effect of the AFB on Huh7 functions.

Our analysis of the 3D cultures has shown a decline of cell growth as compared to the 2D cultures, consistent with results reported previously with other cell types including Huh7.[5,47,48] Only Huh7 cells near the surface of a cell spheroid demonstrate a proliferation capacity, while quiescent cells are present at the center of the spheroid.[5] However, subconfluent cells in the 2D culture show unrestrained proliferative capacity. These differences in cell proliferation capacities in either 2D or 3D systems could explain differences in response to anti-cancer drugs between culture systems. We have demonstrated that 5FU could induce the deterioration of cell growth and apoptosis following 48 h of exposure to 5FU in agreement with previous reports.[14] Notably, after 48 h, the cytotoxic effect of 5FU was more pronounced on highly proliferative cells as 2D system while the potency of 5FU decreased when proliferation was limited as seen in AFB and pellet cultures. In addition, this resistance of the 3D cultures to 5FU might be a result of limited drug diffusion into the aggregates as reported before.[24,49]

According to the results of LDH and calcein AM/PI viability assay, pellet culture clearly showed a decrease in cell integrity early in culture which continued with the course of time. Although the predominate effect of 5FU is shown in proliferating cells, impaired DNA repair, mis-incorporation of 5FU, and subsequent RNA damage could have a large effect on cell survival and metabolism of other quiescent cells.[50] Cell necrosis and apoptosis are both induced by 5FU, but the predominance of one of them is dependent on the cell line

and the 5FU regime used.[14] The high potency of 5FU shown in pellet culture, following 72 h of treatment could not be due to the drug effect without the effect of the aggregation mechanism. The large size of pellets (>500 μm) could result in impaired cell viability, a phenomenon which has been consistently reported[51–53] that may cause a concurrent spontaneous cell death and eventually, decreased viable cell mass available for 5FU. On the other hand, the 2D monolayer had preserved cell mass and could increase the need for a higher concentration of 5FU to demonstrate the effect. Conversely, the discoid thickness of ~60 μm appears not to hinder oxygen/nutrient diffusion in AFB aggregates, and this might explain the relatively constant potency of 5FU in AFB aggregates during culture. We have noticed that the cytotoxicity effect of 5FU was well demonstrated in cells with limited proliferation capacities (as in the AFB or pellets) while its cytostatic effect was shown in highly proliferative cells such as in the 2D monolayer.

CONCLUSIONS

Our findings have demonstrated that AFB could be a good tool for the fabrication of size-controllable discoids. The AFB driven Huh7 cell aggregates showed high viability and their functions reflected their diversion toward differentiation. The hepatoma cell aggregates were found to express high levels of E-cadherin, and aggregate process could not be established without the presence of calcium in culture medium. Relatively short times were needed for the formation of stable aggregates. The AFB generated Huh7 aggregates were relatively uniform and due to rapid diffusion into the aggregate core, their response to anti-cancer was comparable to the standard 2D monolayer system, the factors which favour their use as a model for drug toxicity and screening.

ACKNOWLEDGMENTS

We are grateful to all colleagues in NK group, Faculty of Medicine, University of Southampton and Mechatronics Research group, Faculty of Engineering and Physical Sciences, University of Southampton for their assistance in development and their advice. This work was supported by grants from Liver and Pancreatic Cancer Research & Development Charity and University of Southampton, UK. The authors gratefully acknowledge the financial support for the work from the Engineering and Physical Sciences Research Council (EPSRC) Fellowship (No. EP/L025035/1) to P. Glynne-Jones.

Data supporting this study are openly available from the University of Southampton repository at https://doi.org/10.5258/SOTON/D0719.

REFERENCES

[1]S. C. Ramaiahgari, M. W. den Braver, B. Herpers, V. Terpstra, J. N. Commandeur, B. van de Water, and L. S. Price, Arch. Toxicol. **88**(5), 1083–1095 (2014).
[2]L. Sivertsson, M. Ek, M. Darnell, I. Edebert, M. Ingelman-Sundberg, and E. P. A. Neve, Drug Metab. Dispos. **38**(6), 995–1002 (2010).
[3]B. Sainz, Jr., V. TenCate, and S. L. Uprichard, Virol. J. **6**, 103 (2009).
[4]R. Edmondson, J. J. Broglie, A. F. Adcock, and L. J. Yang, Assay Drug Dev. Technol. **12**(4), 207–218 (2014).
[5]H. R. Jung, H. M. Kang, J. W. Ryu, D. S. Kim, K. H. Noh, E. S. Kim, H. J. Lee, K. S. Chung, H. S. Cho, N. S. Kim, D. S. Im, J. H. Lim, and C. R. Jung, Sci. Rep. **7**(1), 10499 (2017).
[6]R. J. W. Jen-Yin Goh and L. Dixon, "Development and use of in vitro alternatives to animal testing by the pharmaceutical industry 1980-2013," Toxicol. Res. **4**(5), 1297–1307 (2015).
[7]J. Liu, L. A. Kuznetsova, G. O. Edwards, J. Xu, M. Ma, W. M. Purcell, S. K. Jackson, and W. T. Coakley, J. Cell. Biochem. **102**(5), 1180–1189 (2007).
[8]P. Glynne-Jones, R. J. Boltryk, and M. Hill, Lab Chip **12**(8), 1417–1426 (2012).
[9]A. Lenshof, C. Magnusson, and T. Laurell, Lab Chip **12**(7), 1210–1223 (2012).
[10]L. A. Kuznetsova, D. Bazou, and W. T. Coakley, Langmuir **23**(6), 3009–3016 (2007).
[11]U. S. Jonnalagadda, M. Hill, W. Messaoudi, R. B. Cook, R. O. C. Oreffo, P. Glynne-Jones, and R. S. Tare, Lab Chip **18**(3), 473–485 (2018).
[12]J. J. Lei, P. Glynne-Jones, and M. Hill, Phys. Fluids **28**(1), 012004 (2016).
[13]M. Kondo, H. Nagano, H. Wada, B. Damdinsuren, H. Yamamoto, N. Hiraoka, H. Eguchi, A. Miyamoto, T. Yamamoto, H. Ota, M. Nakamura, S. Marubashi, K. Dono, K. Umeshita, S. Nakamori, M. Sakon, and M. Monden, Clin. Cancer Res. **11**(3), 1277–1286 (2005), see http://clincancerres.aacrjournals.org/content/11/3/1277.
[14]O. Brenes, F. Arce, O. Gatjens-Boniche, and C. Diaz, Biomed. Pharmacother. **61**(6), 347–355 (2007).
[15]M. Hill, Y. Shen, and J. J. Hawkes, Ultrasonics **40**(1–8), 385–392 (2002).
[16]R. Krimholtz, D. A. Leedom, and G. L. Matthaei, Electron. Lett. **6**(13), 398 (1970).
[17]S. P. Martin, R. J. Townsend, L. A. Kuznetsova, K. A. J. Borthwick, M. Hill, M. B. McDonnell, and W. T. Coakley, Biosens. Bioelectron. **21**(5), 758–767 (2005).
[18]D. Bazou, L. A. Kuznetsova, and W. T. Coakley, Ultrasound Med. Biol. **31**(3), 423–430 (2005).
[19]D. Bazou, W. T. Coakley, A. J. Hayes, and S. K. Jackson, Toxicol. In Vitro **22**(5), 1321–1331 (2008).
[20]J. Schindelin, I. Arganda-Carreras, E. Frise, V. Kaynig, M. Longair, T. Pietzsch, S. Preibisch, C. Rueden, S. Saalfeld, B. Schmid, J.-Y. Tinevez, D. J. White, V. Hartenstein, K. Eliceiri, P. Tomancak, and A. Cardona, Nat. Methods **9**, 676 (2012).
[21]R. J. Zawada, P. Kwan, K. L. Olszewski, M. Llinas, and S. G. Huang, Biochem. Cell Biol. **87**(3), 541–544 (2009).
[22]S. Kasibhatla, G. P. Amarante-Mendes, D. Finucane, T. Brunner, E. Bossy-Wetzel, and D. R. Green, CSH Protoc. **2006**, 1 (2006).
[23]R. Glicklis, J. C. Merchuk, and S. Cohen, Biotechnol. Bioeng. **86**(6), 672–680 (2004).
[24]K. Chen, M. Wu, F. Guo, P. Li, C. Y. Chan, Z. Mao, S. Li, L. Ren, R. Zhang, and T. J. Huang, Lab Chip **16**(14), 2636–2643 (2016).
[25]S. S. Kantak and R. H. Kramer, J. Biol. Chem. **273**(27), 16953–16961 (1998).
[26]M. Takeichi, Curr. Opin. Cell Biol. **7**(5), 619–627 (1995).
[27]T. Shimada, H. Yamazaki, M. Mimura, Y. Inui, and F. P. Guengerich, J. Pharmacol. Exp. Ther. **270**(1), 414–423 (1994), see http://jpet.aspetjournals.org/content/270/1/414.
[28]F. P. Guengerich, Annu. Rev. Pharmacol. Toxicol. **39**, 1–17 (1999).
[29]U. M. Zanger, M. Turpeinen, K. Klein, and M. Schwab, Anal. Bioanal. Chem. **392**(6), 1093–1108 (2008).
[30]Y. Zhou, K. Yang, J. Cui, J. Y. Ye, and C. X. Deng, J. Control. Release **157**(1), 103–111 (2012).
[31]D. Carugo, D. N. Ankrett, P. Glynne-Jones, L. Capretto, R. J. Boltryk, X. Zhang, P. A. Townsend, and M. Hill, Biomicrofluidics **5**(4), 044108–044115 (2011).
[32]D. Bratosin, L. Mitrofan, C. Palii, J. Estaquier, and J. Montreuil, Cytometry A **66a**(1), 78–84 (2005).
[33]R. Reinehr, S. Becker, A. Hongen, and D. Haussinger, J. Biol. Chem. **279**(23), 23977–23987 (2004).
[34]C. Leroy, C. Colmont, M. Pisam, and G. Rousselet, Eur. J. Cell Biol. **79**(12), 936–942 (2000).
[35]B. K. Straub, S. Rickelt, R. Zimbelmann, C. Grund, C. Kuhn, M. Iken, M. Ott, P. Schirmacher, and W. W. Franke, J. Cell Biol. **195**(5), 873–887 (2011).

[36]B. W. Wong, J. M. Luk, I. O. Ng, M. Y. Hu, K. D. Liu, and S. T. Fan, Biochem. Biophys. Res. Commun. **311**(3), 618–624 (2003).
[37]R.-Z. Lin, L.-F. Chou, C.-C. M. Chien, and H.-Y. Chang, Cell Tissue Res. **324**(3), 411–422 (2006).
[38]D. Bazou, G. A. Foster, J. R. Ralphs, and W. T. Coakley, Mol. Membr. Biol. **22**(3), 229–240 (2005).
[39]A. G. Grieve and C. Rabouille, J. Cell Sci. **127**(Pt 15), 3331–3346 (2014).
[40]M. Wiklund, Lab Chip **12**(11), 2018–2028 (2012).
[41]H. Bohm, P. Anthony, M. R. Davey, L. G. Briarty, J. B. Power, K. C. Lowe, E. Benes, and M. Groschl, Ultrasonics **38**(1–8), 629–632 (2000).
[42]S. Radel, L. Gherardini, A. J. McLoughlin, O. Doblhoff-Dier, and E. Benes, Bioseparation **9**(6), 369–377 (2000).
[43]S. Radel, A. J. McLoughlin, L. Gherardini, O. Doblhoff-Dier, and E. Benes, Ultrasonics **38**(1–8), 633–637 (2000).
[44]D. Bazou, R. Kearney, F. Mansergh, C. Bourdon, J. Farrar, and M. Wride, Ultrasound Med. Biol. **37**(2), 321–330 (2011).
[45]L. Sivertsson, I. Edebert, M. P. Palmertz, M. Ingelman-Sundberg, and E. P. A. Neve, Mol. Pharmacol. **83**(3), 659–670 (2013).
[46]M. Takagi, N. Fukuda, and T. Yoshida, Cytotechnology **24**(1), 39–45 (1997).
[47]W. A. Renner, M. Jordan, H. M. Eppenberger, and C. Leist, Biotechnol. Bioeng. **41**(2), 188–193 (1993).
[48]M. Haji-Karim and J. Carlsson, Cancer Res. **38**(5), 1457–1464 (1978), see http://cancerres.aacrjournals.org/content/38/5/1457.
[49]Y. C. Tung, A. Y. Hsiao, S. G. Allen, Y. S. Torisawa, M. Ho, and S. Takayama, Analyst **136**(3), 473–478 (2011).
[50]D. B. Longley, D. P. Harkin, and P. G. Johnston, Nat. Rev. Cancer **3**(5), 330–338 (2003).
[51]K. Groebe and W. MuellerKlieser, Int. J. Radiat. Oncol. Biol. Phys. **34**(2), 395–401 (1996).
[52]F. Hirschhaeuser, H. Menne, C. Dittfeld, J. West, W. Mueller-Klieser, and L. A. Kunz-Schughart, J. Biotechnol. **148**(1), 3–15 (2010).
[53]S. Y. Ong, H. Dai, and K. W. Leong, Biomaterials **27**(22), 4087–4097 (2006).